CHIN. PHYS. LETT. Vol. 37, No. 9 (2020) 097401

A New Quasi-One-Dimensional Ternary Molybdenum Pnictide $Rb_2Mo_3As_3$ with Superconducting Transition at 10.5 K

Kang Zhao(赵康)[1,2], Qing-Ge Mu(穆青隔)[1,2], Bin-Bin Ruan(阮彬彬)[1,2,3], Meng-Hu Zhou(周孟虎)[1,2,3], Qing-Song Yang(杨清松)[1,2], Tong Liu(刘通)[1,2], Bo-Jin Pan(潘伯津)[1,2], Shuai Zhang(张帅)[1,2], Gen-Fu Chen(陈根富)[1,2,3], and Zhi-An Ren(任治安)[1,2,3*]

[1]*Institute of Physics and Beijing National Laboratory for Condensed Matter Physics, Chinese Academy of Sciences, Beijing 100190, China*
[2]*School of Physical Sciences, University of Chinese Academy of Sciences, Beijing 100049, China*
[3]*Songshan Lake Materials Laboratory, Dongguan 523808, China*

(Received 17 June 2020; accepted 9 July 2020; published online 1 September 2020)

We report superconductivity in a new ternary molybdenum pnictide $Rb_2Mo_3As_3$, synthesized via the solid state reaction method. Powder x-ray diffraction analysis reveals a hexagonal crystal structure with space group $P\bar{6}m2$ (No. 187), and the refined lattice parameters are $a = 10.431(5)$ Å, $c = 4.460(4)$ Å. SEM images show rod-like grains with good ductility, confirming a quasi-one-dimensional (Q1D) structure. Electrical resistivity and dc magnetic susceptibility characterizations exhibit superconductivity with an onset of $T_c = 10.5$ K. The upper critical field of $Rb_2Mo_3As_3$ is estimated to be 28.2 T at zero temperature, providing an evidence of possible unconventional superconductivity. Our recent discovery of MoAs-based superconductors above 10 K provides a unique platform for the study of exotic superconductivity in 4*d* electron systems with Q1D crystal structures.

PACS: 74.70.Dd, 74.62.Bf, 74.70.−b DOI: 10.1088/0256-307X/37/9/097401

Transition metal-based compounds with low-dimensional structures host many intriguing physical phenomena, such as charge density waves (CDWs), heavy fermions, and superconductivity.[1,2] Since high-temperature superconductivity (HTSC) was first discovered in layered cuprates and iron pnictides/chalcogenides, a variety of transition metal-based compounds with typical layered crystal structures have been thoroughly studied in a search for novel superconductors with high transition temperatures (T_c).[3–9] However, there is another family of superconductors, based on the transition metal Mo, i.e., the Chevrel phase, which was discovered earlier than cuprates and iron-based superconductors.[10,11] With a common formula of $M_xMo_6X_8$, the Chevrel phase is composed of unique Mo_6X_8 clusters and the inserted metal element M, forming a three-dimensional lattice. The Chevrel phase possesses relatively high T_c, the highest of which is reported to be 15 K in $PbMo_6S_8$. $PbMo_6S_8$ also exhibits a very high upper critical field ($\mu_0 H_{c2}$), estimated to be higher than 80 T at zero temperature.[11–13] Owing to the pretty high T_c and $\mu_0 H_{c2}$ observed at that time, $PbMo_6S_8$ attracted a great deal of interest in relation to both theoretical and applied research. A multiband order parameter was evidenced by the research of Petrovic *et al.*[13] in 2011, which suggested a strongly coupled quasi-isotropic band coexisting with a highly anisotropic weakly coupled minority band in $PbMo_6S_8$.

Recently, a novel family of CrAs-based superconductors $A_2Cr_3As_3$ (A = Na, K, Rb or Cs) with lower dimensionality have been discovered, comprising special quasi-one-dimensional (Q1D) $(Cr_3As_3)^{2-}$ linear chains, separated by columns of alkali metal cations.[14–17] These Q1D superconductors exhibit non-centrosymmetric crystal structures, and some intriguing characteristics from the perspective of physical property characterizations; possible unconventional spin-triplet superconductivity has also been suggested.[18–24] Superconductivity has also been reported in Q1D-type ACr_3As_3 (A = K, Rb) crystals by removing half of the inter-chain alkali metal ions from $A_2Cr_3As_3$.[25,26] Unlike $A_2Cr_3As_3$, ACr_3As_3 compounds crystallize in a centrosymmetric structure. Interestingly, T_cs in these two families change in opposite trends when the lattice parameters are tuned via the inter-chain alkali metal ions, although they show very similar behaviors in relation to superconducting transition temperature and critical fields.[14–17,25,26] It is also worth mentioning that the origin of superconductivity in the ACr_3As_3 system has recently been suggested to be related to possible electron doping via hydrogen intercalation.[27–29]

The study of Q1D Mo-based superconductors dates from the discovery of $M_2Mo_6X_6$ (M = Tl, In; X = Se) as derivatives from the Chevrel phase, which have identical crystal structures to the ACr_3As_3 compounds.[30–32] Although Mo-based ternary com-

Supported by the National Key Research and Development of China (Grant Nos. 2018YFA0704200 and 2016YFA0300301), the National Natural Science Foundation of China (Grant No. 11774402), and the Strategic Priority Research Program of Chinese Academy of Sciences (Grant No. XDB25000000).
*Corresponding author. Email: renzhian@iphy.ac.cn
© 2020 Chinese Physical Society and IOP Publishing Ltd

pounds have been extensively studied in relation to the occurrence of superconductivity in many molybdenum chalcogenides (Chevrel phase) since the 1970s, the first two MoAs-based ternary superconductors, $K_2Mo_3As_3$ and $Cs_2Mo_3As_3$, were only discovered very recently.[33,34] Both exhibit the unconventional superconductivity with T_c higher than other Q1D superconductors. Here, we report the synthesis and characterizations of a new ternary molybdenum pnictide $Rb_2Mo_3As_3$, and show how the occurrence of superconductivity at 10.5 K was revealed by means of both electrical resistivity and magnetic susceptibility measurements.

Polycrystalline $Rb_2Mo_3As_3$ samples were prepared via the high temperature solid state reaction method, with Rb (lump, 99.75%), Mo (powder, 99.95%), and As (powder, 99.999%) as starting materials. To begin with, the RbAs precursor was prepared based on Rb lumps and As powders with a stoichiometric ratio of 1:1. The mixture was loaded into an alumina crucible and sealed into an evacuated quartz tube, which was then very slowly (4 K/h) heated to 523 K and sintered for 20 hours, followed by cooling down to room temperature in the furnace. Subsequently, the obtained RbAs was ground into a fine powder and mixed thoroughly with Mo and As powders in a stoichiometric ratio of 2.3 : 3 : 0.7 before being pressed into pellets. In this process, the excess Rb used to compensate for volatilization is quite important in order to obtain a single-phase sample. The pellets were placed into an alumina crucible and sealed into an evacuated quartz tube and sintered at 523 K for 20 h. After cooling to room temperature, the product was ground and once again pressed into pellets, placed into an alumina crucible and sealed into a Ta tube. The tube was arc-welded in an argon atmosphere before being sealed into an evacuated quartz tube. The sample was heated at 1123 K for 50 hours prior to being cooled down to room temperature by shutting down the furnace. Eventually, polycrystalline $Rb_2Mo_3As_3$ samples were obtained. The samples are black in color and extremely reactive to both oxygen and moisture, hence all manipulations mentioned above were carried out in a high-purity argon atmosphere, and any exposure to air should be avoided when performing measurements on the samples.

The crystal structure was characterized by powder x-ray diffraction (PXRD) at room temperature on a PAN-analytical x-ray diffractometer with Cu K_α radiation. Rietveld analysis of the PXRD data was performed using the GSAS package. The morphology of the sample surface was investigated with a Phenom scanning electron microscope (SEM). The electrical resistivity measurement was carried out on a Quantum Design physical property measurement system (PPMS) via the standard four-probe method in magnetic fields of up to 9 T. The dc magnetization was measured with a Quantum Design magnetic property measurement system (MPMS) in zero-field-cooled (ZFC) and field-cooled (FC) modes.

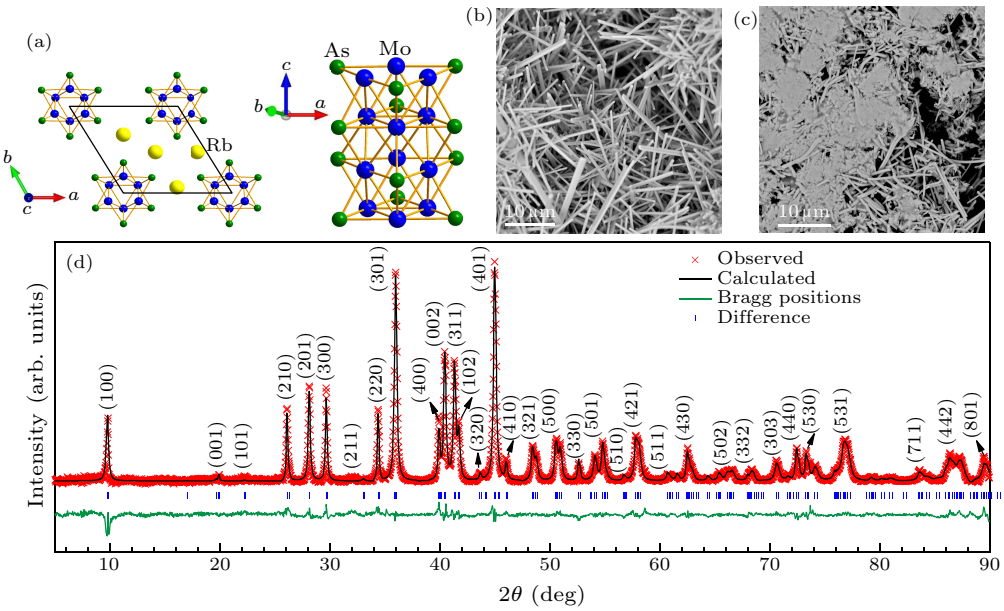

Fig. 1. (a) Structural schematic of $Rb_2Mo_3As_3$. (b) SEM image of the fresh surface of the polycrystalline $Rb_2Mo_3As_3$ sample. (c) SEM image of the $Rb_2Mo_3As_3$ sample surface after pressure treatment. (d) Powder x-ray diffraction pattern and Rietveld refinement data of polycrystalline $Rb_2Mo_3As_3$ sample.

Figure 1(d) shows the typical PXRD pattern collected from 5° to 90° at room temperature. All diffraction peaks were well indexed with space group $P\bar{6}m2$ (No. 187). The SEM image of the sample surface in Fig. 1(b) shows rod-like grains, which reveals the Q1D nature of the crystal structure. Similarly to the previously reported $A_2Cr_3As_3$, $Rb_2Mo_3As_3$ crystallizes in a non-centrosymmetric Q1D structure, where infinite $(Mo_3As_3)^{2-}$ double-walled nanotubes are separated by columns of Rb^+ ions, as depicted

in Fig. 1(a).[14–17,33] Notably, the samples have very good ductility under pressure, which in contrast with iron-arsenide superconductors. Figures 1(b) and 1(c) show a fresh sample surface and a surface after pressure treatment at room temperature, respectively. Most grains twisted into a curled shape and squeezed together without breaking under pressure, as a result of the good ductility of the sample. Rietveld refinement gives the lattice parameters as $a = 10.431(5)$ Å and $c = 4.460(4)$ Å; further crystallographic details are listed in Table 1. Compared with $K_2Mo_3As_3$, the lattice parameters of $Rb_2Mo_3As_3$ extend by 2.8% along the a axis, and only 0.16% along the c axis.[33] For these novel $A_2Mo_3As_3$ (A = K, Rb, Cs) compounds, the cell expands clearly along the a axis, while the c axis changes very slightly with the replacement of alkali cations with larger radii, which is similar to the phenomenon observed with $A_2Cr_3As_3$ compounds, since the inter-chain bonding is dominated by the alkali cations.[14–17]

The typical temperature dependence of electrical resistivity for $Rb_2Mo_3As_3$ is displayed in Figs. 2(a) and 2(b), which illustrate a clear superconducting transition at low temperature. The onset T_c for $Rb_2Mo_3As_3$ is 10.5 K, and the resistivity reaches zero at 9.0 K. Table 1 gives the crystallographic data and superconducting parameters for $K_2Mo_3As_3$, $Rb_2Mo_3As_3$ and $Cs_2Mo_3As_3$. In comparison, the transition temperatures of $K_2Mo_3As_3$ and $Cs_2Mo_3As_3$ are 10.4 K and 11.5 K, respectively, indicating that T_c increases slightly with the replacement of alkali metals with a larger ionic radius. In layered iron-based superconductors, chemical doping/substitution is an effective method for tuning magnetism and superconductivity by regulating the inter-layer spacing and the As-Fe-As bond angle.[35,36] In the case of $A_2Mo_3As_3$, substitution with larger alkali metal cations enlarges the inter-chain distance and weakens the inter-chain bonding, as indicated by the change in lattice parameters. Meanwhile, the expansion of cell volume results in a reduction of the so-called chemical pressure, hence the T_c exhibits a negative chemical pressure effect, contrary to the isostructural $A_2Cr_3As_3$ superconductors, but similar to the 133-type ACr_3As_3 superconductors.[14–17,25,26] The different behaviors of the T_c on the tuning of its crystal structure may reflect the complicated band structures at the Fermi surface in these Cr/Mo based Q1D compounds, which merits further investigation. Figure 2(a) displays the resistivity curve, in a temperature range of 2–300 K. The normal-state temperature dependence of resistivity exhibits a metallic behavior, which monotonically decreases with a reduction in temperature, and the residual resistivity ratio (RRR) is about 1.6. Note that the shape of the R–T curve is quite sensitive to sample quality. Samples kept for a longer time tend to show smaller RRR, indicating poor sample quality due to high reactivity. Even the direct application of silver paste onto the sample results in resistive upturn at low temperatures, since the paste reacts with the samples, a procedure which should be undertaken with caution during measurement.

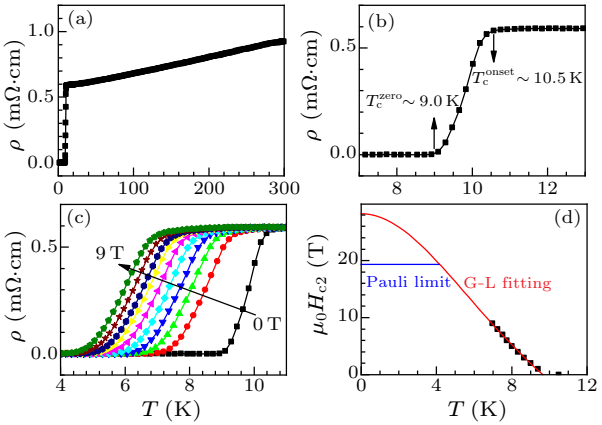

Fig. 2. (a) Temperature dependence of electrical resistivity of the $Rb_2Mo_3As_3$ sample. (b) An enlarged view of the superconducting transition of $Rb_2Mo_3As_3$. (c) R–T curves near superconducting transitions, measured in external magnetic fields of up to 9 T. (d) H_{c2}, fitted via the Ginzburg–Landau theory (red line) and the Pauli paramagnetic limit (blue line) for $Rb_2Mo_3As_3$.

Table 1. Crystallographic data and superconducting parameters of $A_2Mo_3As_3$ (A = K, Rb, Cs).

	$K_2Mo_3As_3$			$Rb_2Mo_3As_3$			$Cs_2Mo_3As_3$		
Space group	$P\bar{6}m2$			$P\bar{6}m2$			$P\bar{6}m2$		
a (Å)	10.145(5)			10.431(5)			10.740(6)		
c (Å)	4.453(8)			4.460(4)			4.463(6)		
V (Å^3)	397.016(6)			420.336(6)			445.748(5)		
T_c (K)	10.4			10.5			11.5		
$\mu_0 H_{c2}(0)$ (T)	22.0			28.2			61.7		
Atoms	x	y	z	x	y	z	x	y	z
As1 ($3j$)	0.8326	0.1674	0	0.8237	0.1763	0	0.8390	0.1610	0
As2 ($3k$)	0.6357	0.8178	0.5	0.6539	0.8269	0.5	0.6705	0.8352	0.5
Mo1 ($3k$)	0.9017	0.0984	0.5	0.9107	0.0893	0.5	0.9134	0.0866	0.5
Mo2 ($3j$)	0.8192	0.9096	0	0.8105	0.9053	0	0.8259	0.9130	0
$A1$ ($3k$)	0.5293	0.0587	0.5	0.5323	0.0646	0.5	0.5379	0.0758	0.5
$A2$ ($1c$)	0.3333	0.6667	0	0.3333	0.6667	0	0.3333	0.6667	0

To characterize the H_{c2} of $Rb_2Mo_3As_3$, electrical resistivity measurements with constant magnetic fields perpendicular to the electrical current were conducted in a temperature range of 2–13 K. The applied

magnetic fields varied from 0 to 9 T with a 1 T interval, and the data are given in Fig. 2(c). The superconducting transition is gradually suppressed to lower temperatures by the magnetic field, with the transition width slightly broadening, and no obvious magnetoresistance effect appears at the normal state. Since the transition width is very sensitive to sample quality, and varies from sample to sample due to the reactive nature of this material, the data extracted from the more stable T_c^{onset}, rather than T_c^{zero} are used to determine $\mu_0 H_{c2}(0)$. In Fig. 2(d), data relating to $\mu_0 H_{c2}$ vs T is fitted using the formula from the Ginzburg–Landau theory, $\mu_0 H_{c2}(T) = \mu_0 H_{c2}(0)(1-t^2)/(1+t^2)$, where t represents T/T_c, giving a $\mu_0 H_{c2}(0)$value of 28.2 T. The T_c under no external magnetic field is excluded when fitting the data, so as to be a better match for the data. The presence of an anisotropic upper critical field has been reported in other Q1D superconducting systems, and for $Rb_2Mo_3As_3$ the possible anisotropy needs to be clarified by measurements of single crystals.[20,30] Nonetheless, this value of $\mu_0 H_{c2}(0)$ exceeds the Pauli paramagnetic limit $\mu_0 H_p = 1.84 T_c = 19.32$ T, similarly to the behavior of $\mu_0 H_{c2}$ in $K_2Mo_3As_3$.[33,37] The behavior of the upper critical field of these samples indicates unconventional superconductivity in Mo-233 type novel superconductors. Spin-triplet pairing has been put forward to explain such behavior in the $A_2Cr_3As_3$ and ACr_3As_3 family, which may also be a possible explanation with regard to these MoAs-based superconductors. Moreover, the existence of the multiband effect may also account for the high $\mu_0 H_{c2}$, as recently reported in relation to these Q1D systems.[19,32,38,39] In order to explore this electron pairing symmetry in greater detail, the fabrication of high-quality $Rb_2Mo_3As_3$ single crystals is of vital importance.

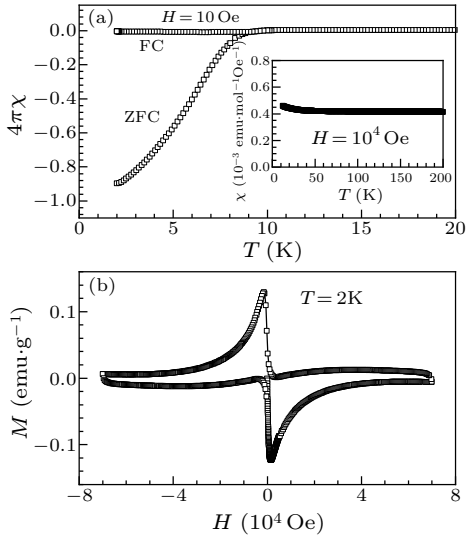

Fig. 3. (a) Low temperature magnetic susceptibility for $Rb_2Mo_3As_3$ measured under 10 Oe. The inset shows the magnetic susceptibility measured under 10000 Oe (black dots), and Curie–Weiss fitting data (red line). (b) Isothermal magnetization curve of $Rb_2Mo_3As_3$ measured from −7 T to 7 T at 2 K.

The temperature-dependent dc magnetic susceptibility from 2 K to 20 K for $Rb_2Mo_3As_3$ with both ZFC and FC measurements under a stable magnetic field of 10 Oe is displayed in Fig. 3. Both ZFC and FC curves show clear diamagnetic signals, associated with superconducting transition at 10.2 K, which agrees well with the T_c value of the electrical resistivity measurements. The magnetic shielding volume fraction derived from the ZFC curve reaches about 90% at 2 K, indicating the effective superconductivity of this compound. In addition, the deviation of the FC curve from the ZFC curve, as a result of the flux pinning effect, indicates typical type-Ⅱ superconductivity. To investigate the normal state magnetism, the magnetic susceptibility in a magnetic field of 1 T was measured and is plotted in the inset of Fig. 3(a). No magnetic phase transition can be seen above T_c. The value of magnetic susceptibility is very small, and the curve is almost independent of temperature. A slight Curie–Weiss-like upturn at low temperature may arise due to magnetic impurities. This indicates that the normal state of $Rb_2Mo_3As_3$ should be that of a Pauli paramagnetic metal.[40] Furthermore, Fig. 3(b) shows the isothermal magnetization loop of the $Rb_2Mo_3As_3$ sample, with the magnetic field ranging from −7 T to 7 T, suggesting typical type-Ⅱ superconductivity with weak flux pinning effect in this compound.

In summary, we have successfully synthesized a new MoAs-based ternary compound $Rb_2Mo_3As_3$, exhibiting a hexagonal Q1D crystal structure, via the solid state reaction method. Electrical resistivity and magnetic susceptibility characterizations reveal the occurrence of superconductivity at a T_c of 10.5 K. These newly discovered $A_2Mo_3As_3$ (A = K, Rb, Cs) superconductors host the highest T_c of all Q1D systems, and their superconductivity exhibits a weak negative chemical pressure effect, in contrast to the previously reported isostructural $A_2Cr_3As_3$ superconductors. Containing the same group VIB transition elements, the discovery of these MoAs-based and CrAs-based superconductors provides a unique platform for studying exotic superconductivity, correlated with 3d and 4d electrons and Q1D structures.

References

[1] Wilson J A, Di Salvo F J and Mahajan S 1975 *Adv. Phys.* **24** 117
[2] Steglich F, Aarts J, Bredl C D *et al.* 1979 *Phys. Rev. Lett.* **43** 1892
[3] Bednorz J G and Muller K A 1986 *Z. Phys. B: Condens. Matter* **64** 189
[4] Wu M K, Ashburn J R, Torng C J *et al.* 1987 *Phys. Rev. Lett.* **58** 908
[5] Kamihara Y, Watanabe T, Hirano M *et al.* 2008 *J. Am. Chem. Soc.* **130** 3296
[6] Rotter M, Tegel M and Johrendt D 2008 *Phys. Rev. Lett.* **101** 107006
[7] Ren Z A, Lu W, Yang J *et al.* 2008 *Chin. Phys. Lett.* **25** 2215
[8] Hsu F C, Luo J Y, Yeh K W *et al.* 2008 *Proc. Natl. Acad. Sci. USA* **105** 14262

[9] Yu J, Liu T, Pan B J *et al.* 2017 *Sci. Bull.* **62** 218
[10] Chevrel R, Sergent M and Prigent J 1971 *J. Solid State Chem.* **3** 515
[11] Peña O 2015 *Physica C* **514** 95
[12] Okuda K, Kitagawa M, Sakakibara T *et al.* 1980 *J. Phys. Soc. Jpn.* **48** 2157
[13] Petrović A P, Lortz R, Santi G *et al.* 2011 *Phys. Rev. Lett.* **106** 017003
[14] Bao J K, Liu J Y, Ma C W *et al.* 2015 *Phys. Rev. X* **5** 011013
[15] Tang Z T, Bao J K, Liu Y *et al.* 2015 *Phys. Rev. B* **91** 020506(R)
[16] Tang Z T, Bao J K, Wang Z *et al.* 2015 *Sci. Chin. Mater.* **58** 16
[17] Mu Q G, Ruan B B, Pan B J *et al.* 2018 *Phys. Rev. Mater.* **2** 034803
[18] Zhong H, Feng X Y, Chen H *et al.* 2015 *Phys. Rev. Lett.* **115** 227001
[19] Watson M D, Feng Y, Nicholson C W *et al.* 2017 *Phys. Rev. Lett.* **118** 097002
[20] Balakirev F F, Kong T, Jaime M *et al.* 2015 *Phys. Rev. B* **91** 220505(R)
[21] Luo J, Yang J, Zhou R *et al.* 2019 *Phys. Rev. Lett.* **123** 047001
[22] Wu X X, Yang F, Le C C *et al.* 2015 *Phys. Rev. B* **92** 104511
[23] Luo J, Wang C, Wang Z *et al.* 2020 *Chin. Phys. B* **29** 067402
[24] Cao G H and Zhu Z W 2018 *Chin. Phys. B* **27** 107401
[25] Mu Q G, Ruan B B, Pan B J *et al.* 2017 *Phys. Rev. B* **96** 140504(R)
[26] Liu T, Mu Q G, Pan B J *et al.* 2017 *Europhys. Lett.* **120** 27006
[27] Taddei K M, Sanjeewa L D, Lei B H *et al.* 2019 *Phys. Rev. B* **100** 220503(R)
[28] Xiang J J, Yu Y L, Wu S Q *et al.* 2019 *Phys. Rev. Mater.* **3** 114802
[29] Wu S Q, Cao C and Cao G H 2019 *Phys. Rev. B* **100** 155108
[30] Potel M, Chevrel R and Sergent M 1980 *J. Solid State Chem.* **35** 286
[31] Armici J C, Decroux M, Fischer O *et al.* 1980 *Solid State Commun.* **33** 607
[32] Petrović A P, Lortz R, Santi G *et al.* 2010 *Phys. Rev. B* **82** 235128
[33] Mu Q G, Ruan B B, Zhao K *et al.* 2018 *Sci. Bull.* **63** 952
[34] Zhao K, Mu Q G, Ruan B B *et al.* 2020 *APL Mater.* **8** 031103
[35] Luo X G and Chen X H 2015 *Sci. Chin. Mater.* **58** 77
[36] Stewart G R 2011 *Rev. Mod. Phys.* **83** 1589
[37] Clogston A M 1962 *Phys. Rev. Lett.* **9** 266
[38] Liu Z X, Chen M Y, Xiang Y *et al.* 2019 *Phys. Rev. B* **100** 094511
[39] Gurevich A 2003 *Phys. Rev. B* **67** 184515
[40] Wang H, Dong C, Mao Q *et al.* 2013 *Phys. Rev. Lett.* **111** 207001